# Structural and Vibrational Properties of Liquid Water from van der Waals Density Functionals

Cui Zhang,[†] Jun Wu,[‡] Giulia Galli,*,[†,§] and François Gygi[‡,‖]

[†]Department of Chemistry, University of California, Davis, California 95616, United States

[‡]Department of Applied Science, University of California, Davis, California 95616, United States

[§]Department of Physics, University of California, Davis, California 95616, United States

[‖]Department of Computer Science, University of California, Davis, California 95616, United States

Ⓢ *Supporting Information*

**ABSTRACT:** We present results for the structural and vibrational properties of the water molecule, water dimer, and liquid water at the experimental equilibrium density, as obtained with several van der Waals density functionals. The functional form originally proposed by Dion et al. [*Phys. Rev. Lett.* **2004**, *92*, 246401], with an appropriately chosen local exchange functional, yields a description of the liquid superior to that of the semilocal functional PBE. In particular, a specific choice of the local exchange functional (optB88) fitted to quantum chemistry calculations yields the best agreement with experimental results for pair correlation functions although it is slightly inferior to other van der Waals functionals in describing infrared spectra. When using optB88, liquid water displays a hydrogen-bonded network less tightly bound than when using the PBE approximation. The performance of optB88 is definitely inferior to that of the PBE0 hybrid functional for the isolated molecule but only moderately so for the liquid. However, the computational cost of optB88 is much less than that of hybrid functionals; therefore the use of optB88 appears to be a sensible alternative to calculations implying the evaluation of the Fock operator, in cases when simulations of large systems are required.

## 1. INTRODUCTION

In the past two decades, much progress has been reported in simulations of liquid water from first principles.[1] However, discrepancies with experimental data remain, when using calculations based on density functional theory (DFT), e.g., in describing the structural and diffusive properties of the system. One issue that is receiving much attention lately is the performance of van der Waals density functionals[2−4] (vdW-DFs) in predicting the properties of water; these are functionals designed to account for dispersion forces, at least approximately.

van der Waals forces denote the forces between atoms or molecules in dilute gases or liquids, i.e., in the presence of negligible electronic charge overlap between the constituents. According to several authors, for example ref 5, for point-like polar molecules, one may identify three different contributions to vdW forces: (i) thermal orientation, originating from dipole−dipole interactions, first described by Keesom;[6,7] (ii) induction, stemming from dipole-induced dipole interactions, introduced by Debye;[8,9] and (iii) dispersion, first discussed by London,[10] arising from the dynamic interactions between fluctuating dipoles. The first two contributions are present only in systems whose building blocks have a permanent dipole (and thus in water), while the third one occurs between any type of atoms or molecules, irrespective of their polarity. In all three cases, the interaction energies decay as the sixth power of the distance.

In liquid water, there is a non-negligible electronic charge overlap between first neighbor molecules, whose main interaction is through hydrogen bonding, not vdW forces. Many definitions have been given of hydrogen bonding,[11] including a recent one by IUPAC;[12] for the purpose of the present discussion, we loosely define a hydrogen bond (HB) as the attractive interaction between a proton donor covalently bonded to a species X (X−H) and a proton acceptor Y.[11] Both charge transfer (CT) effects and electrostatic interactions contribute to hydrogen bonding. A recent analysis of the relative contribution of these two components in the water dimer has been given by Khaliullin et al.,[13] who showed that the amount of intermolecular CT is on the order of a few millielectrons, i.e., much smaller than inferred from conventional population analysis in the past. In the liquid, most of the vdW interaction energy comes from second neighbor molecules, but a small contribution is expected also from non-hydrogen bonded configurations between first neighbors, originating from geometries where both charge overlap and CT are much smaller than in HBs. In these configurations, oxygen−oxygen distances roughly correspond to the first minimum of the oxygen−oxygen pair correlation function.

To understand the performance of semilocal and hybrid density functionals (e.g., those derived within generalized gradient approximations (GGA) such as PBE,[14,15] BLYP,[16,17] and PBE0[18]) in describing the induction and orientation contributions to vdW forces, it is useful to examine how well these functionals can account for the dipole moment ($\mu$) of water molecules in ice and water. In the gas phase, the dipole moment of the molecule has been measured to great accuracy: it is 1.855 D,[19] and most DFTs can reproduce this values within 3% (see section 3.1). The same quantity in condensed phases is not well-defined and thus cannot be measured, since it is not possible to partition in a unique way the electronic charge density between individual molecules. However, the quantity $\mu^2 G$ can be derived from the measured

dielectric constant ($\varepsilon_0$); within linear response, $\mu^2 G = 3k_B T(\varepsilon_0 - 1)/4\pi\rho$, where $\rho$ and $T$ are the number density and temperature of the system, respectively, and $k_B$ is the Boltzmann constant. $G$ is a correlation factor that accounts for angular correlations among dipoles: $G = 1 + \Sigma_i N_i \langle \cos\theta_i \rangle$, where $N_i$ is the number of molecules in the $i$th coordination shell and $\langle \cos\theta_i \rangle$ is the average cosine of the angle between the dipole of a given molecule and a dipole in the $i$th coordination shell ($G = 1$ for uncorrelated dipoles). For perfectly ordered ice, $G = 3$, and thus at ambient conditions, for proton disordered ice, one expects $G \leq 3$, implying $\mu \geq 3.03$ D for $\varepsilon_0 \simeq 107$.[20] Experimental estimates for liquid water, based on X-ray form factors, yield $\mu = 2.9 \pm 0.6$.[21] One may also estimate an effective dipole moment of molecules in ice and water from calculations of the induced dipole on a given molecule due to its environment, based on electrostatics. Such calculations were pioneered by Coulson and Eisenberg,[22] who used a self-consistent induction model to obtain the dipole moment of a water molecule in ice. Using values of the quadrupole moment of the isolated molecule available at the time, and a series of approximations including the neglect of intermolecular polarizability, Coulson and Eisenberg obtained a value of 2.6 D (often misquoted as the dipole moment of the molecule in liquid water or even as an experimental result). Twenty years later, Batista et al.[23] used a model similar to that of ref 22, but they employed refined values of the multipole moments of the isolated molecule and computed a value of 3.09 D, which is most probably a lower bound to the dipole moment in ice.

Within a first principle approach based on ab initio molecular dynamics, where both ice and water are considered as condensed systems, one may define an effective dipole moment from maximally localized Wannier functions[24] (MLWFs). These are derived from linear combinations of Bloch states, obtained by self-consistent solutions of the Kohn−Sham equations. Four doubly occupied MLWFs may be associated with each molecule (there are eight valence electrons per molecule) and $\vec{\mu}$ is computed as[25] $\vec{\mu} = q\vec{r}_{H_1} + q\vec{r}_{H_2} + 6q\vec{r}_O - 2q\Sigma_{c=1}^{4} \vec{r}_{wc}$, where $\vec{r}_{wc}$, $c = 1$ to 4 are the four maximally localized Wannier centers (MLWCs). On average, the overlap between MLWFs of adjacent molecules is less than 1% of the norm.[25] When using experimental equilibrium density, the PBE approximation yields a dipole moment of water equal to $3.24 \pm 0.31$ D and $3.09 \pm 0.34$ D at ~325 K and ~439 K,[26] respectively, and a dipole moment of ice Ih equal to 3.32 D at 273 K.[27] The PBE0 approximation yields slightly lower values ($3.09 \pm 0.28$ D at ~330 K and $2.94 \pm 0.30$ D at ~438 K[26]). These all appear to be physically sound figures, indicating that induction and orientation forces in water and ice should be described in a reasonable manner by these DFTs.

The description of dispersion forces is much more delicate and implies the ability to account for complex electronic correlation effects. The contribution of dispersion forces to the binding of water is expected to be small compared to that of hydrogen bonding. For example, using the formula $C_6 R^{-6}$ with $C_6$ taken from the recent estimates of Grimme et al.[28] and $R$ equal to the average second neighbor distance (as from the second peak of the experimental $g_{OO}(R)$), and assuming that the largest contribution to dispersion comes from the second neighbors (about 10 on average in liquid water), one obtains ~0.01 eV; this interaction energy is ~20 times smaller than the HB energy in the water dimer (0.24 eV[29]). Although weak, dispersion forces may influence the fine details of the potential energy surface of liquid water and possibly its equilibrium density.

Attempts to include dispersion forces in ab initio simulations of liquid water fall into two categories: one strategy consists of adding $C_6 R^{-6}$ dispersion-like terms or dispersion-corrected atom-centered potentials (DCACP) to the potential energy surface obtained with semilocal DFTs:[30] $E_{DFT-D} = E_{DFT} + E_{disp}$.[31,32] Another strategy is based on the use of so-called vdW-DFs[2] designed to include, in an approximate manner, correlation effects responsible for London dispersion forces. We note that vdW-DFs not only include a partial description of dispersion forces but also provide different results for induction and orientation terms, with respect to PBE and PBE0, as well as for hydrogen bonding and intramolecular covalent bonding. Therefore, a comparison of results obtained with GGA functionals and with hybrid functionals and those obtained with vdW-DFs does not provide a direct measure of the importance of dispersion forces in water. (Unfortunately, much confusion is present in this issue in the literature.) Schemes adding $C_6 R^{-6}$ and higher terms onto the energy obtained with GGA functionals could in principle provide a clearer separation between dispersion and HB contributions to the binding of liquid water; however, such a distinction ultimately relies on the choice of a cutoff distance at which a vdW term is added to the Hamiltonian, and this choice is by no means straightforward, especially in molecular dynamics simulations.

Recently, it has been shown[33,34] that the use of the empirical correction proposed by Grimme together with the BLYP functional (BLYP-D) gives a better agreement with experimental results for the computed equilibrium density of the liquid (0.992 g/cm³) and the computed melting temperature (~360 K instead of ~400 K) at the experimental equilibrium density. However, the second peak of the oxygen−oxygen pair correlation function appears to be washed out,[34,35] and the estimated oxygen coordination number is very large (7.1).[35] The average number of HBs is instead reasonable, ~3.45.[35] The use of a DCACP in conjuction with the BLYP functional gives a better agreement with experimental results in terms of correlation functions and 4.6, 3.61, and $2.91 \pm 0.28$ D for the oxygen coordination number, average number of HBs, and dipole moment[35] at ~325 K, respectively. The use of self-consistent polarization density functional theory (SCP-DFT) proposed by Murdachaew et al.[36] gives instead an oxygen−oxygen pair correlation function slightly more overstructured than that with BLYP and a slightly larger oxygen coordination number (4.4 vs 4.1). However, harmonic vibrational frequencies and interaction energies of water clusters are in better agreement with experimental results than those obtained with BLYP.

The performance of some vdW-DFs for the structure and density of liquid water was recently addressed by Wang et al.,[37] using localized basis sets and the SIESTA code. The use of the vdW-DF originally proposed by Dion et al.[2] with the choice of the PBE exchange fucntionals appears to give a softening of the liquid structure with respect to PBE and to experimental results, and a significant improvement on the equilibrium density and diffusivity of the liquid at room temperature (1.13 g/cm³ and 0.208 Å²/ps to be compared with experimental values 1.11 g/cm³ and 0.18 Å²/ps of heavy water). However, if the revPBE exchange is adopted in the definition of vdW-DF, in ref 37, a collapse of the second coordination shell of the liquid is observed.

In this paper, we present an assessment of the performance of several vdW-DFs recently proposed in the literature to describe liquid water at the experimental equilibrium density using pseudopotentials and plane wave basis sets. We show that the vdW-DF recently proposed by Klimeš et al.[4] gives results in better

agreement with experimental results for the structural properties of water than the vdW-DFs originally proposed by Lee et al.[38] and Wang et al.[37] and of basically the same quality for the vibrational properties. Hereafter, we refer to the functional introduced in ref 4 as optB88; all functionals are defined in detail in the following section. The quality of the agreement with experimental results for optB88 is superior to the one obtained with PBE; however, it is slightly inferior to that obtained with PBE0 for the vibrational properties. This indicates that the optB88 functional may provide a promising framework to study water solvation properties of ions and water in contact with surfaces when large supercells are required.

The rest of the paper is organized as follows: in section 2, we describe our theoretical and computational frameworks, and in section 3, we present our results for the water molecule, dimer, and liquid water. Our summary and conclusions are given in section 4.

## 2. METHODS

We performed calculations of the structural and vibrational properties of the water molecule and dimer and first principles molecular dynamics (MD) simulations of 32 heavy water molecules at a fixed density of 1.108 g/cm$^3$ using the Qbox code.[39] We compared the results obtained with semilocal (PBE) and hybrid (PBE0) functionals with those of four different vdW-DFs, which we denote by the following acronyms: DRSLL,[2] DRSLLPBE,[37] LMKLL,[38] and optB88;[4] these are defined in detail below. In vdW-DFs, the exchange correlation energy is defined as

$$E_{xc} = E_x^{GGA} + E_c^{LDA} + E_c^{nl} \qquad (1)$$

where $E_x^{GGA}$ is the exchange energy as defined for GGA functionals, $E_c^{LDA}$ is the local correlation energy obtained within the local density approximation (LDA), and $E_c^{nl}$ is the nonlocal correlation energy, expressed as

$$E_c^{nl} = \frac{1}{2} \int d^3 \vec{r} \int d^3 \vec{r}'\, n(\vec{r})\, \phi(\vec{r}, \vec{r}')\, n(\vec{r}') \qquad (2)$$

The kernel $\phi$ is a universal function[2] which depends on $\vec{r}$ and $\vec{r}'$ through the variables $d = |\vec{r} - \vec{r}'| q_0(\vec{r})$ and $d' = |\vec{r} - \vec{r}'| q_0(\vec{r}')$, and it must be evaluated numerically. $q_0(\vec{r})$ is the central quantity of vdW-DFs; it is a function of the density and the density gradient, given by

$$q_0(\vec{r}) = k_F(\vec{r}) \frac{\varepsilon_{xc}^0(\vec{r})}{\varepsilon_x^{LDA}(\vec{r})} \qquad (3)$$

In eq 3, $k_F(\vec{r}) = [3\pi^2 n(\vec{r})]^{1/3}$ is the local Fermi wave vector and

$$\varepsilon_{xc}^0(\vec{r}) \approx \varepsilon_{xc}^{LDA}(\vec{r}) - \varepsilon_x^{LDA}(\vec{r}) \left[ \frac{Z_{ab}}{9} \left( \frac{\nabla n(\vec{r})}{2 k_F(\vec{r}) n(\vec{r})} \right)^2 \right] \qquad (4)$$

The four vdW-DFs used here differ by the choice of $E_x^{GGA}$ in eq 1 and by the screening factor $Z_{ab}$ in eq 4. Three of the functionals adopted here contain the same $E_c^{nl}$ as originally proposed in ref 2, except for LMKLL, where the screening factor $Z_{ab}$ is changed from −0.8491 to −1.887. The $E_x^{GGA}$ is different in each functional. In the original vdW-DF (DRSLL) proposed in refs 2 and 40, $E_x^{GGA}$ is computed with the revPBE[41] exchange functional. The recently proposed functionals DRSLLPBE and LMKLL replace the revPBE exchange functional with the PBE and

**Table 1. Selelcted Properties of the Water Molecule, As Computed with Different Density Functionals**[a]

| | $\nu_1$ | $\nu_2$ | $\nu_3$ | $r_{OH}$ | $\angle$HOH | $\mu$ |
|---|---|---|---|---|---|---|
| PBE | 3692 | 1592 | 3801 | 0.972 | 104.3 | 1.811 |
| PBE0 | 3834 | 1638 | 3946 | 0.961 | 104.8 | 1.861 |
| DRSLL | 3663 | 1618 | 3769 | 0.971 | 104.5 | 1.801 |
| DRSLLPBE | 3661 | 1608 | 3767 | 0.972 | 104.5 | 1.807 |
| LMKLL | 3636 | 1623 | 3741 | 0.971 | 104.8 | 1.800 |
| optB88 | 3663 | 1604 | 3770 | 0.973 | 104.4 | 1.813 |
| PBEPBE[b] | 3702 | 1601 | 3804 | 0.971 | 104.1 | 1.813 |
| PBE1PBE[b] | 3862 | 1643 | 3965 | 0.959 | 104.8 | 1.862 |
| Expt. | 3832[c] | 1648[c] | 3943[c] | 0.957[51] | 104.5[51] | 1.855[19] |

[a] $\nu$ denotes vibrational frequencies in cm$^{-1}$. $\nu_1$ is the symmetric stretching. $\nu_2$ is the bending, and $\nu_3$ is the asymmetric stretching frequency. $r_{OH}$, $\angle$HOH, and $\mu$ are the bond length in Å, bond angle in degrees, and molecular dipole moment in Debye, respectively. Calculations were carried out in a cubic cell with $L = 30$ Bohr and a kinetic energy cutoff of 100 Ry. The converged value of the dipole moment was obtained by linear extrapolation of results obtained with cells of $L = 30$, 40, 50, 60, and 70 Bohr, as a function of $1/L$. [b] All electron calculations.[49] [c] Experimental harmonic frequencies.[51]

PW86[42,43] exchange, respectively. In the optB88 functional, an alternative optimized exchange functional B88[16] is proposed; the exchange enhancement factor of the B88 functional originally proposed by Becke[16] is

$$F_x^{B88}(s) = 1 + \mu s^2 / (1 + \beta s\, \text{arcsinh}(cs)) \qquad (5)$$

where $c = 2^{4/3}(3\pi^2)^{1/3}$, $\mu \cong 0.2743$, and $\beta = 9\,\mu(6/\pi)^{1/3}/2c$. Klimeš et al.[4] suggested to modify the ratio $\mu/\beta$ so as to optimize the binding energies of the molecules belonging to the S22 data set, as obtained using CCSD(T) calculations. Such an optimal ratio turns out to be $\mu/\beta = 1.2$ with $\mu = 0.22$, yielding ∼10 meV mean absolute deviation for the interaction energies of the S22 data set. The calculation of the nonlocal correlation functional in the Qbox code was carried out by transforming the costly double integral of the kernel function $\phi$ into an efficient direct sum of Fourier coefficients as proposed in ref 44. Additional details of the implementation, including an efficient handling of the divergence of $\phi$ at the origin, will be given elsewhere.

We used plane wave basis sets and norm-conserving pseudopotentials (of the HSCV type[45,46]) with a kinetic energy cutoff of 85 Ry. Simulations were carried out with a time step of 10 au (0.24 fs) in the NVE ensemble, within the Born–Oppenheimer approximation, and trajectories were collected for 20 ps for each run. The electronic contributions to the molecular dipole moment were computed using MLWFs, evaluated at each MD step with the algorithm proposed in ref 47. The IR absorption coefficient per unit length was obtained within linear response theory from the Fourier transform of the time correlation function of the system's dipole moment:[48]

$$\alpha(\omega) = \frac{2\pi\omega^2 \beta}{3cVn(\omega)} \int_{-\infty}^{\infty} dt\, e^{-i\omega t} \left\langle \sum_{ij} \vec{\mu_i}(0) \cdot \vec{\mu_j}(t) \right\rangle \qquad (6)$$

where $n(\omega)$ is the refractive index, $V$ is the volume, $\beta = 1/k_B T$ is the inverse temperature, and $\vec{\mu}_i$ is the molecular dipole moment. In the next section, we discuss the performance of the vdW-DFs defined above for liquid water, after a brief discussion of the results obtained for the isolated water molecule and the dimer.

3056

dx.doi.org/10.1021/ct200329e |J. Chem. Theory Comput. 2011, 7, 3054–3061

**Table 2. Vibrational Frequencies of the Water Dimer $(H_2O)_2{}^a$**

|  | $\nu_1$ | $\nu_2$ | $\nu_3$ | $\nu_4$ | $\nu_5$ | $\nu_6$ | $d_{OO}$ | $r_{OH}^D$ | $\angle O \cdots OH$ |
|---|---|---|---|---|---|---|---|---|---|
| PBE | 3686 | 1591 | 3792 | 3526 | 1610 | 3769 | 2.895 | 0.982 | 6.2 |
| PBE0 | 3838 | 1658 | 3946 | 3707 | 1637 | 3925 | 2.886 | 0.970 | 5.4 |
| DRSLL | 3662 | 1631 | 3764 | 3589 | 1616 | 3744 | 3.022 | 0.976 | 5.6 |
| DRSLLPBE | 3656 | 1606 | 3757 | 3546 | 1622 | 3736 | 2.924 | 0.980 | 6.6 |
| LMKLL | 3634 | 1619 | 3735 | 3543 | 1635 | 3712 | 2.967 | 0.978 | 5.9 |
| optB88 | 3638 | 1601 | 3760 | 3529 | 1619 | 3737 | 2.909 | 0.982 | 5.8 |
| PBEPBE[b] | 3695 | 1600 | 3795 | 3536 | 1621 | 3773 | 2.899 | 0.981 | 6.3 |
| PBE1PBE[b] | 3853 | 1644 | 3952 | 3720 | 1665 | 3935 | 2.896 | 0.968 | 5.9 |
| Expt. | 3797[c] | 1653[c] | 3899[c] | 3718[c] | 1669[c] | 3881[c] | 2.976[52] | - | 6 ± 20[52] |

$^a$ $\nu$ denotes vibrational frequencies in cm$^{-1}$. $\nu_1$ is the symmetric stretching of the acceptor. $\nu_2$ is the bending of the acceptor. $\nu_3$ is the asymmetric stretching of the acceptor. $\nu_4$ is the symmetric stretching of the donor. $\nu_5$ is the bending of the donor, and $\nu_6$ is the asymmetric stretching of the donor. $d_{OO}$ is the oxygen−oxygen distance in Å. $r_{OH}^D$ (Å) is the OH bond length of the donor. $\angle O \cdots OH$ (degree) is the angle between the oxygen−oxygen distance and the OH bond of the donor. Calculations were carried out in a cubic cell with $L = 60$ Bohr and a kinetic energy cutoff 100 Ry. $^b$ All electron calculations.[49] $^c$ Experimental harmonic frequencies.[53]
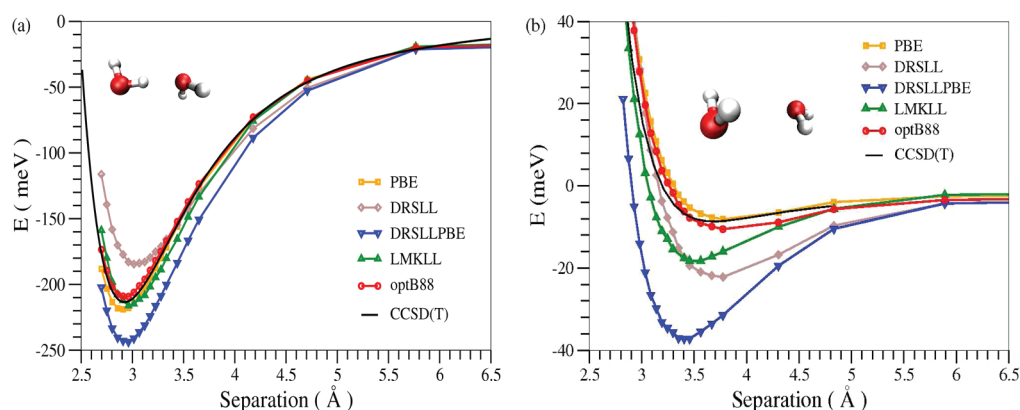


**Figure 1.** Interaction energy of the water dimer as a function of the separation of the water molecule center of mass, calculated with the DRSLL (gray), DRSLLPBE (blue), LMKLL (green), optB88 (red), and PBE functionals (orange). (a) Hydrogen-bonded configuration. The CCSD(T) curve[54] is showed by the black line. (b) Non-hydrogen-bonded configuration. The CCSD(T) curve, shown in black, is extrapolated to the complete basis set limit following the same procedure described in ref 55. All plane-wave calculations were carried out in a cubic cell with $L = 60$ Bohr and a kinetic energy cutoff of 100 Ry.

## 3. RESULTS AND DISCUSSION

**3.1. Water Molecule and Water Dimer.** Table 1 shows the results obtained for the structural and vibrational properties of the isolated water molecule with different functionals. PBE0 is superior to all other functionals and yields the best results for the molecule, as compared to experimental results. In particular, the average error in vibrational frequencies is 0.3%, smaller than the one obtained with PBE (3.6%) and the vdW-DFs ($\geq 3.5\%$); the PBE0 dipole moment is in excellent agreement with experimental result while all other functionals underestimate it by at least 2.3%. The bending mode of the molecule is reproduced slightly better by the vdW-DFs than by PBE, while the opposite is true for the stretching modes. The results with the PBE and PBE0 functionals obtained here for the water molecule are in excellent agreement with those reported by Xu et al.,[49] who carried out calculations with highly accurate Gaussian basis sets. Table 2 shows the intramolecular vibrational frequencies of the dimer. We find the same trend when the functional is changed as that of the isolated molecule, except for the symmetric stretching mode of the donor that is reproduced better by vdW-DFs.

Figure 1a and b show the binding curves of a hydrogen-bonded dimer (HBD) and a non-hydrogen bonded dimer (NHBD),

respectively. For the hydrogen bonded one, we used the same dimer geometry as the one optimized in quantum chemistry (QC) calculations at the CCSD(T) level;[50] the non-hydrogen-bonded configuration was extracted from a liquid water simulation, and it is representative of oxygen−oxygen distances close to the first minimum of the $g_{OO}(r)$. PBE, optB88, and LMKLL functionals all give a binding energy and a binding curve of the HBD in good agreement with that of CCSD(T), while DRSLL and DRSLLPBE yield an underestimate and overestimate of the binding, respectively. Non-hydrogen-bonded configurations appear to be much more favored by DRSLL, with respect to hydrogen-bonded ones, than by all other functionals. PBE and optB88 functional calculations best reproduce CCSD(T) results for the NHBD, although the repulsive part of the curve is slightly stiffer than that of the CCSD(T) curve.

**3.2. Liquid Water.** Several properties of liquid water obtained with the various functionals described in section 3.2 are summarized in Table 3. Oxygen−oxygen pair correlation functions are given in Figure 2a and b, respectively, where it is seen that the best agreement with experimental results is obtained with the optB88 functional, in simulations at $\simeq 326$ K, although the differences in performance with respect to DRSLLPBE appear to be minor. In particular, although the first maximum is at a distance

**Table 3. Properties of Liquid Water Computed with Several van der Waals Functionals and Semilocal and Hybrid Functionals[a]**

| | $T$ (K) | $\mu$ (D) | $N_{Hbonds}$ | $r_{max}$ (Å) | $g_{OO}(r_{max})$ | $r_{min}$ (Å) | $g_{OO}(r_{min})$ | $N_{Coord.}$ |
|---|---|---|---|---|---|---|---|---|
| DRSLLPBE | $295 \pm 20$ | $2.93 \pm 0.25$ | $3.56 \pm 0.8$ | 2.80 | 2.77 | 3.34 | 0.71 | 4.34 |
| LMKLL | $291 \pm 20$ | $2.83 \pm 0.23$ | $3.42 \pm 0.8$ | 2.84 | 2.54 | 3.56 | 0.94 | 5.53 |
| LMKLL$_{200}$ | $276 \pm 18$ | $2.82 \pm 0.24$ | $3.43 \pm 0.8$ | 2.87 | 2.65 | 3.52 | 0.91 | 5.30 |
| LMKLL | $237 \pm 16$ | $2.89 \pm 0.23$ | $3.62 \pm 0.7$ | 2.86 | 2.98 | 3.38 | 0.80 | 4.57 |
| optB88 | $282 \pm 19$ | $3.10 \pm 0.28$ | $3.75 \pm 0.6$ | 2.76 | 3.37 | 3.34 | 0.50 | 4.24 |
| optB88 | $326 \pm 24$ | $3.00 \pm 0.29$ | $3.54 \pm 0.8$ | 2.78 | 2.83 | 3.33 | 0.73 | 4.30 |
| PBE | $297 \pm 20$ | $3.27 \pm 0.31$ | $3.84 \pm 0.5$ | 2.71 | 3.67 | 3.24 | 0.28 | 3.98 |
| PBE0 | $330 \pm 24$ | $3.09 \pm 0.28$ | $3.70 \pm 0.7$ | 2.68 | 3.01 | 3.31 | 0.58 | 4.37 |

[a] All results have been obtained with a kinetic energy cutoff of 85 Ry, except for LMKLL$_{200}$, for which 200 Ry was used. $T$, $\mu$ and $N_{Hbonds}$ are the average temperature, average molecular dipole moment, and average number of hydrogen bonds, respectively. $r_{max}$ and $g_{OO}(r_{max})$ are the position and height of the first maximum in $g_{OO}(r)$. $r_{min}$ and $g_{OO}(r_{min})$ are the position and height of the first minimum in $g_{OO}(r)$. $N_{Coord.}$ is the oxygen coordination number. Hydrogen bonds are defined by a geometrical criterion: $d_{OO} < 3.35$ Å and $\angle O \cdots OH < 30°$.
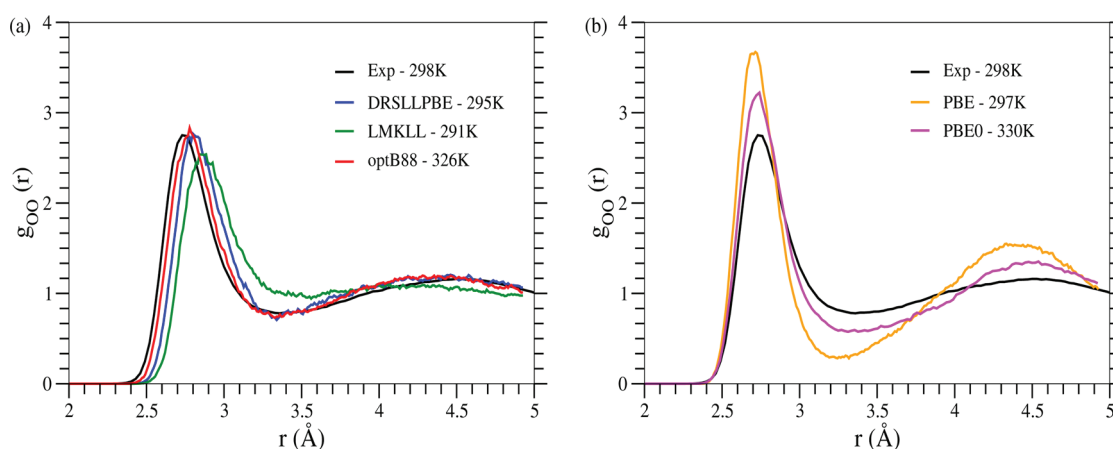


**Figure 2.** (a) Comparison of the oxygen—oxygen pair correlation functions calculated with vdW-DFs: DRSLLPBE at $295 \pm 20$ K (blue), LMKLL at $291 \pm 20$ K (green), and optB88 at $326 \pm 24$ K (red). (b) Comparison of the oxygen—oxygen pair correlation functions obtained with the PBE functional at $297 \pm 20$ K (orange) and the PBE0 functional at $330 \pm 24$ K (magenta). The experimental result[56] at room temperature is displayed by the black line in both a and b.
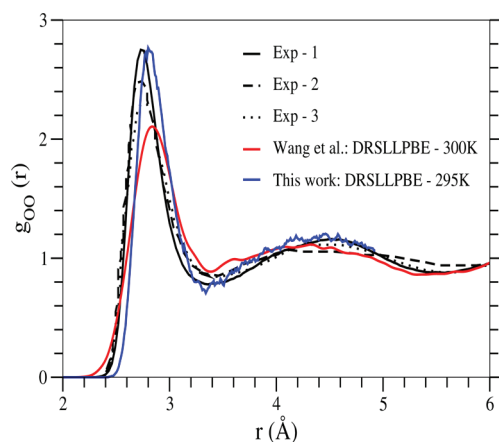


**Figure 3.** Comparison of the oxygen—oxygen pair correlation functions calculated with the DRSLLPBE functional in this work (blue), in ref 37 (red), and the experimental results of ref 56 (solid black), ref 57 (dashed black), and ref 58 (dotted black).

about 0.1 Å larger than in the experimental results, the position of the first minimum and the second maximum are in reasonably good agreement with those of the measured $g_{OO}(r)$ at 298 K. The

LMKLL functional gives instead the worst oxygen—oxygen pair correlation function when compared to experimental results and an unphysically large number of HBs ($>5$) above the experimental melting temperature ($\geq 276$ K); however the number of HBs is decreased to 4.57, if the temperature is lowered to $\sim 237$ K. A comparison of oxygen—oxygen pair correlation functions obtained with LMKLL and optB88 at different temperatures indicates that different vdW-DFs may have rather different computed melting temperatures (see Figures 1 and 2 in the Supporting Information). Our results for the diffusion coefficient are not fully converged given the MD cell sizes used here. However, they clearly indicate that the optB88 functional at 326 K has a self-diffusion constant in much better agreement with experimental results than that of simulations performed with the PBE functional at a similar temperature.

Results for the structural properties of water with the DRSLLPBE functional have also been reported in ref 37. The agreement between those results and ours is only fair, as shown in Figure 3 for the $g_{OO}(r)$. We expect these differences to originate from the use of different basis sets. We note that the accuracy of plane wave basis sets can be easily checked by varying just one parameter, as was done in the case of one of our simulations (see Table 3), where it is shown that results with 85 and 200 Ry are identical, within error bars (see Figure 1 in the Supporting
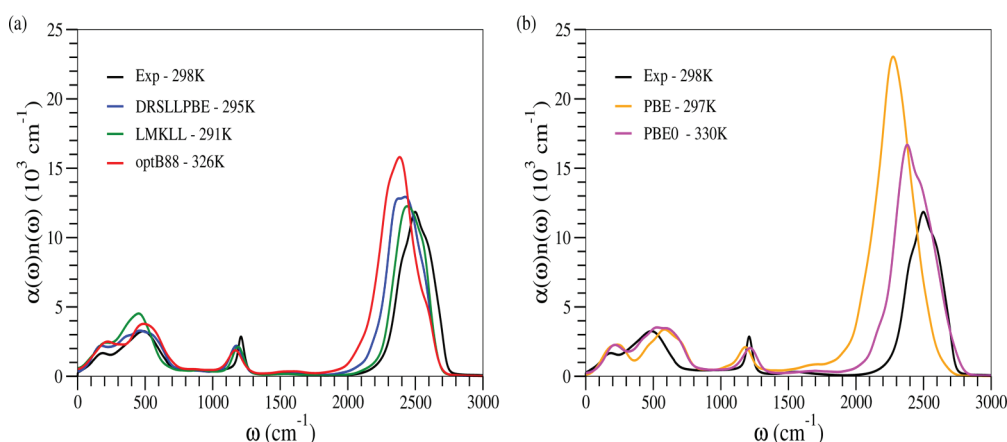
**Figure 4.** (a) Calculated IR spectra of liquid $D_2O$ with vdW-DFs: DRSLLPBE at 295 ± 20 K (blue), LMKLL at 291 ± 20 K (green), and optB88 at 326 ± 24 K (red). (b) Calculated IR spectra of liquid $D_2O$ with the PBE functional at 297 ± 20 K (orange) and the PBE0 functional at 330 ± 24 K (magenta). The experimental result[59] at room temperature is displayed by the black line in both a and b.
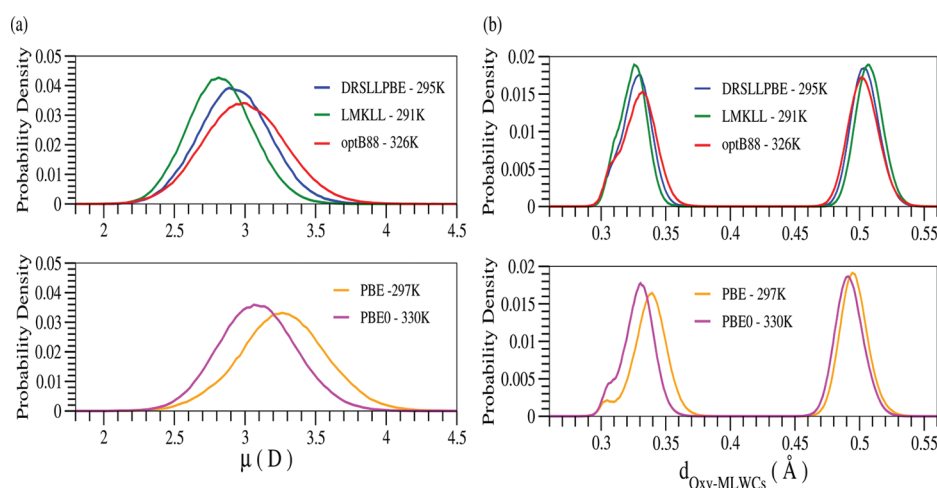


**Figure 5.** (a) Distributions of molecular dipole moments calculated with vdW-DFs: DRSLLPBE at 295 ± 20 K (blue), LMKLL at 291 ± 20 K (green), and optB88 at 326 ± 24 K (red; upper panel) and with the PBE functional at 297 ± 20 K (orange) and the PBE0 functional at 330 ± 24 K (magenta; lower panel). (b) Distributions of distances between oxygen and maximally localized Wannier centers (MLWCs) calculated with vdW-DFs: DRSLLPBE at 295 ± 20 K (blue), LMKLL at 291 ± 20 K (green), and optB88 at 326 ± 24 K (red; upper panel) and with the PBE functional at 297 ± 20 K (orange) and the PBE0 functional at 330 ± 24 K (magenta; lower panel).

Information). We have also checked our results against those of accurate Gaussian calculations for the monomer and dimer (see section 3.1) and found excellent agreement. Such a comparison for the geometry and frequencies of the isolated $H_2O$ and $(H_2O)_2$ molecules computed with the basis sets of the SIESTA code is not available.

The IR spectra obtained with vdW-DFs appear to be superior to the spectrum computed at the PBE level and slightly superior to that computed within PBE0 for the stretching band (see Figure 4a and b). We note that the bending band is in the right position only in the PBE0 simulation. The average dipole moment in the liquid is similar when using optB88 and PBE0 (see Figure 5a), while it turns out to be sizably smaller with DRSLLPBE and LMKLL. Likewise, the distributions of MLWCs are very similar when using optB88 and the hybrid functional (see Figure 5b).

We have also computed the electronic band gaps of the liquid with the different functionals. The ones computed with PBE and the vdW-DFs (obtained as an average over 22 configurations

over 20 ps) are about the same ($\simeq 4.05-4.35 \pm 0.176$ eV), whereas the one obtained with PBE0 is much larger ($\simeq 7.08 \pm 0.189$ eV). Although these are to be taken only as indicative values, as the cells used here are rather small and only the $\Gamma$ point has been used to sample the Brillouin zone, the trend as a function of the chosen functional is significant. In particular, these results indicate that the effective polarizability of the molecule in the fluid is equally overestimated by PBE and the vdW-DFs, while much less so by PBE0. This is consistent with the values obtained for the polarizability of the isolated molecule within PBE and PBE0, 1.542 and 1.412, respectively, as compared to the experimental result of 1.427.[49]

## 4. CONCLUSIONS

The first principles description of the properties of liquid water is an ongoing challenge, originating from the presence of several different bonding configurations which are not equally

3059

dx.doi.org/10.1021/ct200329e |*J. Chem. Theory Comput.* 2011, 7, 3054–3061

well described by any of the known functionals. Accounting for the properties of the liquid encompasses describing with comparable accuracy intramolecular covalent/ionic bonds, intermolecular hydrogen bonds, and vdW interactions. In addition, intermolecular interactions include forces between nonbonded first neighbor molecules: these are unique bonding configurations (e.g., not present in ice at ambient conditions), with small but most likely non-negligible electronic overlap between molecular charge densities. It is clearly a formidable task to account for all of these different bonding configurations with the same level of accuracy; for example, even those functionals providing a good description of intramolecular forces and of hydrogen bonds may still fail in giving the right energy differences between hydrogen-bonded and non-hydrogen-bonded first neighbor molecules. Therefore, cancellation of errors between different configurations explored by the liquid is much more difficult to achieve in water than in a simpler system, where similar bonds are explored during time evolution. Thus, an accurate description of even the simplest properties of water, e.g., structure and diffusivity, remains elusive.

In this work, we have shown that one may find vdW-DFs of the form originally proposed by Dion et al., with appropriately chosen parameters for the local exchange, that give a description of the structural and vibrational properties of the liquid superior to that of the semilocal functional PBE. These findings indicate that the functional form for the correlation energy suggested in ref 2 is physically sound to describe water. However, our results cannot provide a direct measure of the importance of dispersion forces in liquid water. As mentioned in the Introduction, vdW-DFs do not only include an approximate description of dispersion forces (contrary to semilocal functionals that do not include any nonlocal correlations) but also give different descriptions of intramolecular and hydrogen bonds, and of the induction and orientation contributions to vdW energies, with respect to PBE.

In particular, we have shown that the optB88 functional yields the best agreement with experimental results for structure and vibrations and a liquid which displays a hydrogen-bonded network less tightly bound than so-called PBE water at the measured equilibrium density. The optB88 vdW-DF has the same form of the nonlocal correlation energy as that proposed by Dion et al.; however, the revPBE functional used in ref 2 has been substituted by the B88 exchange, reparametrized to fit the binding energies of the S22 data set, as computed with CCSD(T). Similar to the local density approximation (LDA) of DFT, where a functional form of the local correlation was chosen and fitted to the results of a highly accurate calculation (quantum Monte Carlo (QMC)) for the electron gas, the optB88 functional is derived by fitting a given functional form to highly accurate QC calculations (CCSD(T)) for molecules. It is reasonable to expect that even more accurate functionals may be derived, based on Dion et al.'s functional form, if high level calculations (either QC or QMC) become available for an ensemble of relevant systems.

The results obtained here with the optB88 functional are close to those obtained by replacing the revPBE exchange in Dion et al.'s functional with the PBE exchange. Our findings with the latter functional differ from those reported in ref 37, most likely because of the use of different basis sets. Our plane wave basis has been extensively tested for the liquid, by comparing results obtained with two different energy cutoffs, as well as for the isolated molecule and dimer, by comparing with the results of highly accurate Gaussian basis set calculations.

Although the optB88 and DRSLLPBE functionals yield satisfactory results for liquid water at around room temperature, their

performance with respect to the hybrid functional PBE0 depends on the properties: oxygen–oxygen pair correlation fuctions are less overstructured than with PBE0, but the position of the maximum is slightly larger than in the experiment. The IR stretching bands are moderately improved, but the bending bands are inferior to that obtained with PBE0. In addition, these functionals perform worse than PBE0 for the molecule and dimer. However, the computational cost of vdW-DFs is much less than that of hybrid functionals, and therefore they are a sensible alternative to calculations implying the evaluation of the Fock operator, in cases when large systems are required.

## ■ ASSOCIATED CONTENT

Ⓢ **Supporting Information.** Calculated oxygen–oxygen pair correlation functions with the LMKLL and optB88 functionals for systems consisting of 32 water molecules. This material is available free of charge via the Internet at http://pubs.acs.org/.

## ■ AUTHOR INFORMATION

**Corresponding Author**
*E-mail: gagalli@ucdavis.edu.

## ■ ACKNOWLEDGMENT

## ■ REFERENCES

(1) A brief review has been given, for example, in the introduction of: Zhang, C.; Donadio, D.; Gygi, F.; Galli, G. *J. Chem. Theory Comput.* **2011**, *7*, 1443–1449.

(2) Dion, M.; Rydberg, H.; Schröder, E.; Langreth, D. C.; Lundqvist, B. I. *Phys. Rev. Lett.* **2004**, *92*, 246401.

(3) Langreth, D. C.; et al. *J. Phys.: Condens. Matter* **2009**, *21*, 084203.

(4) Klimeš, J.; Bowler, D. R.; Michaelides, A. *J. Phys.: Condens. Matter* **2010**, *22*, 022201.

(5) van Oss, C. J.; Chaudhury, M. K.; Good, R. J. *Chem. Rev.* **1988**, *88*, 927–941.

(6) Keesom, W. H. *Phys. Z.* **1921**, *22*, 129.

(7) Keesom, W. H. *Phys. Z.* **1921**, *22*, 643.

(8) Debye, P. *Phys. Z.* **1920**, *21*, 178.

(9) Debye, P. *Phys. Z.* **1921**, *22*, 302.

(10) London, F. *Z. Phys.* **1930**, *63*, 245–279.

(11) A brief review has been given, for example, in: Buckingham, A. D.; Del Bene, J. E.; McDowell, S. A. C. *Chem. Phys. Lett.* **2008**, *463*, 1–10.

(12) Arunan, E. *Curr. Sci.* **2007**, *92*, 17–18.

3060

dx.doi.org/10.1021/ct200329e |*J. Chem. Theory Comput.* 2011, 7, 3054–3061

(13) Khaliullin, R. Z.; Bell, A. T.; Head-Gordon, M. *Chem.—Eur. J.* **2009**, *15*, 851–855.

(14) Perdew, J. P.; Burke, K.; Ernzerhof, M. *Phys. Rev. Lett.* **1996**, *77*, 3865–3868.

(15) Perdew, J. P.; Burke, K.; Ernzerhof, M. *Phys. Rev. Lett.* **1997**, *78*, 1396.

(16) Becke, A. D. *Phys. Rev. A* **1988**, *38*, 3098–3100.

(17) Lee, C.; Yang, W.; Parr, R. G. *Phys. Rev. B* **1988**, *37*, 785–789.

(18) Adamo, C.; Barone, V. *J. Chem. Phys.* **1999**, *110*, 6158–6170.

(19) Shostak, S. L.; Ebenstein, W. L.; Muenter, J. S. *J. Chem. Phys.* **1991**, *94*, 5875–5882.

(20) Johari, G. P.; Whalley, E. *J. Chem. Phys.* **1981**, *75*, 1333–1340.

(21) Badyal, Y. S.; Saboungi, M.-L.; Price, D. L.; Shastri, S. D.; Haeffner, D. R.; Soper, A. K. *J. Chem. Phys.* **2000**, *112*, 9206–9208.

(22) Coulson, C. A.; Eisenberg, D. *Proc. R. Soc. London, Ser. A* **1966**, *291*, 445–453.

(23) Batista, E. R.; Xantheas, S. S.; Jónsson, H. *J. Chem. Phys.* **1998**, *109*, 4546–4551.

(24) Marzari, N.; Vanderbilt, D. *Phys. Rev. B* **1997**, *56*, 12847–12865.

(25) Silvestrelli, P. L.; Parrinello, M. *Phys. Rev. Lett.* **1999**, *82*, 3308–3311.

(26) Zhang, C.; Donadio, D.; Gygi, F.; Galli, G. *J. Chem. Theory Comput.* **2011**, *7*, 1443–1449.

(27) Sharma, M.; Resta, R.; Car, R. *Phys. Rev. Lett.* **2007**, *98*, 247401.

(28) Grimme, S.; Ehrlich, S.; Goerigk, L. *J. Comput. Chem.* **2011**, *32*, 1456–1465.

(29) Curtiss, L. A.; Frurip, D. J.; Blander, M. *J. Chem. Phys.* **1979**, *71*, 2703–2711.

(30) Tkatchenko, A.; Scheffler, M. *Phys. Rev. Lett.* **2009**, *102*, 073005.

(31) Grimme, S. *J. Comput. Chem.* **2004**, *25*, 1463–1473.

(32) Grimme, S. *J. Comput. Chem.* **2006**, *27*, 1787–1799.

(33) Schmidt, J.; VandeVondele, J.; Kuo, I.-F. W.; Sebastiani, D.; Siepmann, J. I.; Hutter, J.; Mundy, C. J. *J. Phys. Chem. B* **2009**, *113*, 11959–11964.

(34) Yoo, S.; Xantheas, S. S. *J. Chem. Phys.* **2011**, *134*, 121105.

(35) Lin, I.-C.; Seitsonen, A. P.; Coutinho-Neto, M. D.; Tavernelli, I.; Rothlisberger, U. *J. Phys. Chem. B* **2009**, *113*, 1127–1131.

(36) Murdachaew, G.; Mundy, C. J.; Schenter, G. K. *J. Chem. Phys.* **2010**, *132*, 164102.

(37) Wang, J.; Román-Pérez, G.; Soler, J. M.; Artacho, E.; Fernández-Serra, M.-V. *J. Chem. Phys.* **2011**, *134*, 024516.

(38) Lee, K.; Murray, E. D.; Kong, L.; Lundqvist, B. I.; Langreth, D. C. *Phys. Rev. B* **2010**, *82*, 081101.

(39) Qbox code. http://eslab.ucdavis.edu/software/qbox (accessed May 5, 2011).

(40) Thonhauser, T.; Cooper, V. R.; Li, S.; Puzder, A.; Hyldgaard, P.; Langreth, D. C. *Phys. Rev. B* **2007**, *76*, 125112.

(41) Zhang, Y.; Yang, W. *Phys. Rev. Lett.* **1998**, *80*, 890.

(42) Perdew, J. P.; Yue, W. *Phys. Rev. B* **1986**, *33*, 8800–8802.

(43) Murray, E. D.; Lee, K.; Langreth, D. C. *J. Chem. Theory Comput.* **2009**, *5*, 2754–2762.

(44) Román-Pérez, G.; Soler, J. M. *Phys. Rev. Lett.* **2009**, *103*, 096102.

(45) Pseudopotential Table. http://fpmd.ucdavis.edu/potentials (accessed May 5, 2011).

(46) Vanderbilt, D. *Phys. Rev. B* **1985**, *32*, 8412–8415.

(47) Gygi, F.; Fattebert, J. L.; Schwegler, E. *Comput. Phys. Commun.* **2003**, *155*, 1–6.

(48) Ramírez, R.; López-Ciudad, T.; Kumar-P, P.; Marx, D. *J. Chem. Phys.* **2004**, *121*, 3973–3983.

(49) Xu, X.; Goddard, W. A. *J. Phys. Chem. A* **2004**, *108*, 2305–2313.

(50) Jurečka, P.; Šponer, J.; Černy, J.; Hobza, P. *Phys. Chem. Chem. Phys.* **2006**, *8*, 1985–1993.

(51) Benedict, W. S.; Gailar, N.; Plyler, E. K. *J. Chem. Phys.* **1956**, *24*, 1139–1165.

(52) Odutola, J. A.; Dyke, T. R. *J. Chem. Phys.* **1980**, *72*, 5062–5070.

(53) Fredin, L.; Nelander, B.; Ribbegard, G. *J. Chem. Phys.* **1977**, *66*, 4065–4072.

(54) Molnar, L. F.; He, X.; Wang, B.; Merz, K. M. *J. Chem. Phys.* **2009**, *131*, 065102.

(55) Bukowski, R.; Szalewicz, K.; Groenenboom, G. C.; van der Avoird, A. *J. Chem. Phys.* **2008**, *128*, 094313.

(56) Soper, A. K. *Chem. Phys.* **2000**, *258*, 121–137.

(57) Soper, A. K. *J. Phys.: Condens. Matter* **2007**, *19*, 335206.

(58) Hura, G.; Russo, D.; Glaeser, R. M.; Head-Gordon, T.; Krack, M.; Parrinello, M. *Phys. Chem. Chem. Phys.* **2003**, *5*, 1981–1991.

(59) Max, J.-J.; Chapados, C. *J. Chem. Phys.* **2009**, *131*, 184505.

3061

dx.doi.org/10.1021/ct200329e |*J. Chem. Theory Comput.* 2011, 7, 3054–3061